Eur. Phys. J. C 51, 585–591 (2007)
DOI 10.1140/epjc/s10052-007-0327-2

THE EUROPEAN PHYSICAL JOURNAL C

Regular Article – Theoretical Physics

SANCnews: Sector $4f$, charged current[a]

A. Arbuzov[1b], D. Bardin[2], S. Bondarenko[1], P. Christova[2], L. Kalinovskaya[2], G. Nanava[3], R. Sadykov[2], W. von Schlippe[4]

[1] Bogoliubov Laboratory of Theoretical Physics, JINR, Dubna, 141980 Russia
[2] Dzhelepov Laboratory of Nuclear Problems, JINR, Dubna, 141980 Russia
[3] IFJ, PAN, Krakow, Poland
[4] PNPI, St. Petersburg, 188300 Russia

Received: 5 March 2007 /
Published online: 12 June 2007 –

Abstract. In this paper we describe the implementation of the charged current decays of the type $t \to bl^+\nu_l(\gamma)$ in the framework of the SANC system. All calculations are done taking into account the one-loop electroweak correction in the standard model. The emphasis of this paper is on the presentation of numerical results. Various distributions are produced by means of a Monte Carlo integrator and event generator. Comparison with the results of the CompHEP and PYTHIA packages are presented for the Born and hard photon contributions. The validity of the cascade approximation at one-loop level is also studied.

PACS. 14.65.Ha; 12.15.-y; 12.15.Lk

1 Introduction

In this paper we describe a further application of the computer system SANC *Support of Analytic and Numerical calculations for experiments at Colliders* intended for semi-automatic calculations of realistic observables and pseudo-observables for various processes of elementary particle interactions at the one-loop precision level (see [1] and references therein).

Here we concentrate on the implementation of the 4 leg decay $t \to b + l^+ + \nu_l$ as a typical example of the charged current (CC) decay of the type $F \to f + f_1 + \bar{f}_1'$, where F and f stand for massive fermions and f_1 and $\bar{f}_1'$ for massless fermions. In this paper we continue to present the physical applications of the SANC system, started in [2], rather than present the extension of the system itself as continued in [3].

According to the SM the dominant channel of top quark decay is $t \to bW^+$ with a branching ratio of 99.9%. The decay branching ratio of the W boson into leptons is $\mathrm{Br}(W \to l^+\nu_l) \approx 11\%$ [4]. Therefore, the semileptonic decays $t \to bl^+\nu_l$ ($l^+ \equiv e^+$, μ^+, τ^+) amount to approximately 1/3 of all top quark decays.

This paper is devoted to the complete one-loop QED and EW radiative corrections (EWRC) to the 4 leg semileptonic top quark decay $t \to bl^+\nu_l(\gamma)$. The calculation of QCD corrections in SANC for these 3 and 4 leg top decays is presented in [5, 6].

EW and QCD radiative corrections to the 3 leg decay $t \to bW^+$ were first calculated in [7–9], and relevant issues may be found in [10–16]; even two-loop QCD corrections are known [17–19]. However, we are not aware of papers in which the 4 leg top decay $t \to bl^+\nu_l$ would be considered at one loop.

The results for the Born level decay width, presented in this paper, are compared with the calculation performed by means of the CompHEP [20] and PYTHIA [21] packages and those for 5 leg accompanying bremsstrahlung with the results of CompHEP. We also discuss briefly how our results for the one-loop EW corrections are compared with results existing in the literature. The validity of the cascade approximation is also studied.

The paper is organized as follows. In Sect. 2 we briefly recall the calculational scheme adopted in SANC. The Born level is given in Sect. 3 and the one-loop EW corrections in Sect. 4. Various numerical results are collected in Sect. 5. In Sect. 6 we discuss the cascade approach to the problem, and in Sect. 7 we present some conclusions. We assume that the reader may run SANC as described in Sect. 6 of [1] in order to see all relevant formulae that are not presented in this paper and get the corresponding numbers.

[a] This work is partly supported by INTAS grant No. 03-51-4007 and by the EU grant mTkd-CT-2004-510126 in partnership with the CERN Physics Department and by the Polish Ministry of Scientific Research and Information Technology grant No. 620/E-77/6.PRUE/DIE 188/2005-2008

[b] e-mail: arbuzov@theor.jinr.ru

2 Calculation scheme

Recall that SANC performs calculations starting from the construction of EW form factors (FF) that parameterize the covariant amplitude (CA) and helicity amplitudes (HA) of a process. From HA, the s2n software produces the FORTRAN codes for them and then the differential decay width is computed numerically. These codes can further be used in MC generators and integrators. The amplitudes (CA and HA) for the 4 leg top and antitop decays are presented in [1].

These two ingredients, together with accompanying bremsstrahlung (BR) are accessible via the menu sequence SANC → EW → Processes → 4legs → $4f$ → Chargedcurrent → $t \to b\,l\,nu \to t \to b\,l\,nu$(FF, HA, BR); see Fig. 1. A FORM [22] module, loaded at the end of this chain computes on-line the FF, HA and BR, respectively. For more details, see Sect. 2.5 of the SANC description in [1] and [23].

The total one-loop width, $\Gamma^{\text{1-loop}}$, of the decay $t \to bl^+\nu_l(\gamma)$ can be subdivided into the following terms:

$$\Gamma^{\text{1-loop}} = \Gamma^{\text{Born}} + \Gamma^{\text{virt}}(\lambda) + \Gamma^{\text{real}}(\lambda,\bar{\omega}),$$
$$\Gamma^{\text{real}}(\lambda,\bar{\omega}) = \Gamma^{\text{soft}}(\lambda,\bar{\omega}) + \Gamma^{\text{hard}}(\bar{\omega}). \quad (1)$$

Here Γ^{Born} is the decay width in the Born approximation, Γ^{virt} is the virtual contribution, and Γ^{soft} and Γ^{hard} are the contributions due to the soft and hard photon emission, respectively. The auxiliary parameter $\bar{\omega}$ separates the soft and hard photon contributions, and the parameter λ (the "photon mass"), which enters the virtual and soft contributions, regularizes the infrared divergences.

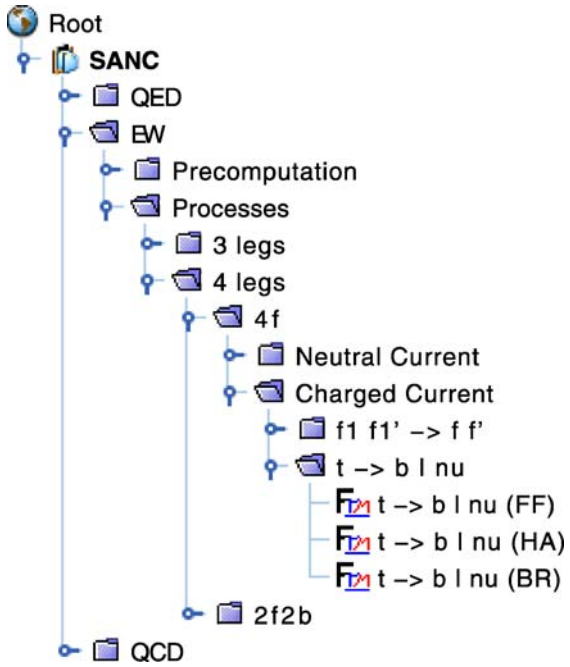

Fig. 1. SANC tree for $t \to bl^+\nu_l$ decay

We here present numbers, collected for the standard SANC INPUT, PDG (2006) [24]:

$$G_{\text{F}} = 1.16637 \times 10^{-5}\,\text{GeV}^{-2}, \quad \alpha(0) = 1/137.03599911$$
$$M_W = 80.403\,\text{GeV}, \quad \Gamma_W = 2.141\,\text{GeV},$$
$$M_Z = 91.1876\,\text{GeV}, \quad \Gamma_Z = 2.4952\,\text{GeV},$$
$$M_H = 120\,\text{GeV}, \quad m_e = 0.51099892 \times 10^{-3}\,\text{GeV},$$
$$m_u = 62\,\text{MeV}, \quad m_d = 83\,\text{MeV},$$
$$m_\mu = 0.105658369\,\text{GeV}, \quad m_c = 1.5\,\text{GeV},$$
$$m_s = 215\,\text{MeV}, \quad m_\tau = 1.77699\,\text{GeV},$$
$$m_b = 4.7\,\text{GeV}, \quad m_t = 174.2\,\text{GeV}. \quad (2)$$

The coupling constants can be set to different values according to the different input parameter schemes. They can be directly identified with the fine-structure constant $\alpha(0)$ together with $e/g = s_W$ and $c_W = M_W/M_Z$. This choice is called the α scheme. Another one, the G_{F} scheme, makes use of the Fermi constant and the quantity Δr. Note that we do not iterate the equation for Δr. We use both schemes to produce the numbers.

3 Born level process

In the Born approximation there is only one Feynman diagram for the decay $t \to bl^+\nu_l$ with one intermediate virtual W^+ boson; see Fig. 2.

The differential decay rate reads

$$\mathrm{d}\Gamma^{\text{Born}} = \frac{1}{2m_t}\overline{\sum_{\text{spins}}}|\mathcal{M}^{\text{Born}}|^2\,\mathrm{d}\Phi^{(3)}, \quad (3)$$

where $\mathcal{M}^{\text{Born}}$ is the amplitude of the process and $\mathrm{d}\Phi^{(3)}$ is the differential three-body phase space:

$$\mathrm{d}\Phi^{(3)} = \Phi_1^{(2)}\,\mathrm{d}\Phi_2^{(2)}\frac{\mathrm{d}s}{2\pi}, \quad (4)$$

expressed in terms of the two-body phase spaces:

$$\Phi_1^{(2)} = \frac{1}{8\pi}\frac{\sqrt{\lambda(m_t^2, m_b^2, s)}}{m_t^2},$$
$$\mathrm{d}\Phi_2^{(2)} = \frac{1}{8\pi}\frac{\sqrt{\lambda(s, m_l^2, 0)}}{s}\frac{1}{2}\mathrm{d}\cos\theta. \quad (5)$$

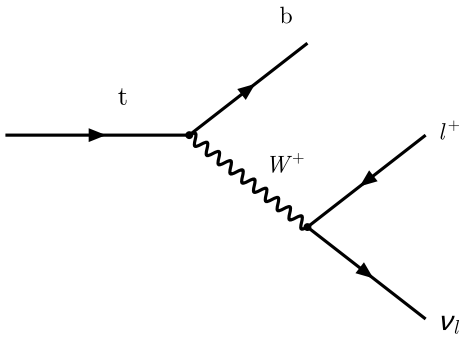

Fig. 2. Feynman diagram for Born level process

One can express the values $|\mathcal{M}^{\rm Born}|^2$ and $d\Phi^{(3)}$ via two independent variables: $s=-(p_l+p_\nu)^2$ and $\cos\theta$, where θ is the angle between p_l and p_b in the rest frame of the compound (l^+,ν_l). The limits of variation are

$$m_l^2 \le s \le (m_t-m_b)^2\,, \qquad -1\le\cos\theta\le+1\,. \tag{6}$$

If the lepton mass is not ignored, then the s and ϑ dependence of the Mandelstam variables t and u is given by

$$(t,u)=m_b^2+m_l^2+\frac{1}{2s}\Big[\left(s+m_l^2\right)\left(m_t^2-m_b^2-s\right) \mp\left(s-m_l^2\right)\sqrt{\lambda_s}\cos\theta\Big], \tag{7}$$

where $\lambda_s=(m_t^2+m_b^2-s)^2-4m_b^2m_t^2$.

The result of the two-fold Monte Carlo integration is shown in Table 1. This calculation is performed by means of a Monte Carlo integration routine based on the VEGAS algorithm [25]. The numbers produced with the help of the CompHEP and PYTHIA packages are also presented in the table.

The results of SANC and CompHEP are in good agreement; the deviation from PYTHIA appears to be due to the difference in the definition of the EW constants. In addition to integration we use a Monte Carlo generator of unweighted events to produce the differential distributions. In Fig. 3 we present some of these distributions and a comparison with distributions, obtained with the help of the CompHEP and PYTHIA packages. We note that the input parameters for this comparison were tuned to CompHEP. In Figs. 3 and 4 we show a triple comparison for the four distributions over various kinematical variables at the Born level. The figures demonstrate very good agreement between SANC and CompHEP and fair agreement with PYTHIA.

Table 1. Born level decay width for decay $t\to b\mu^+\nu_\mu$ produced by SANC, CompHEP and PYTHIA

$\Gamma^{\rm Born}$, GeV		
SANC	CompHEP	PYTHIA
0.16936(1)	0.16935(1)	0.16782(1)

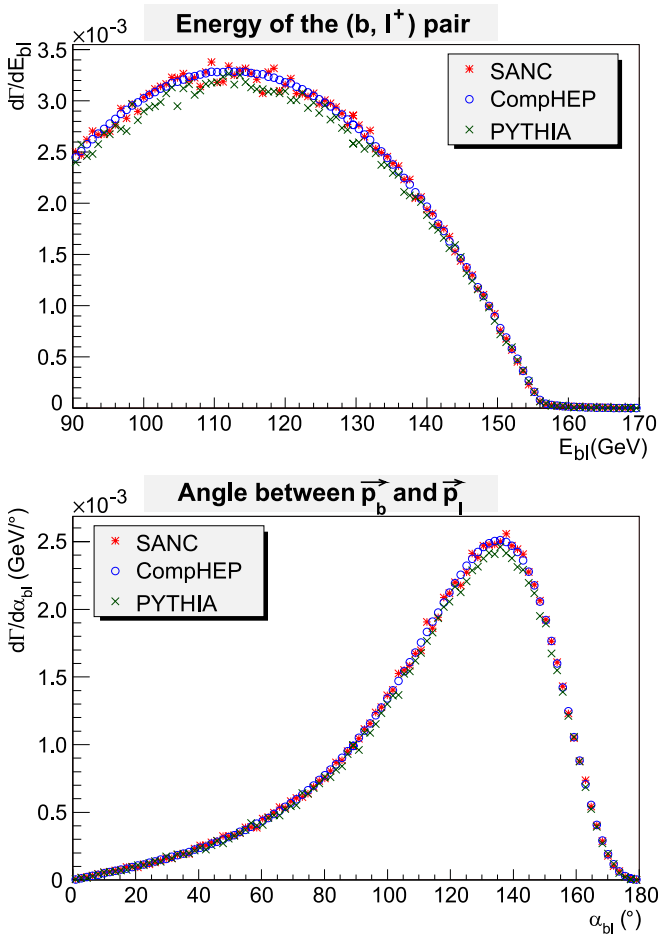

Fig. 3. Differential distributions for the process $t\to b\mu^+\nu_\mu$ of the $b\mu^+$ pair energy and the angle between p_b and p_l produced with the help of SANC, CompHEP and PYTHIA

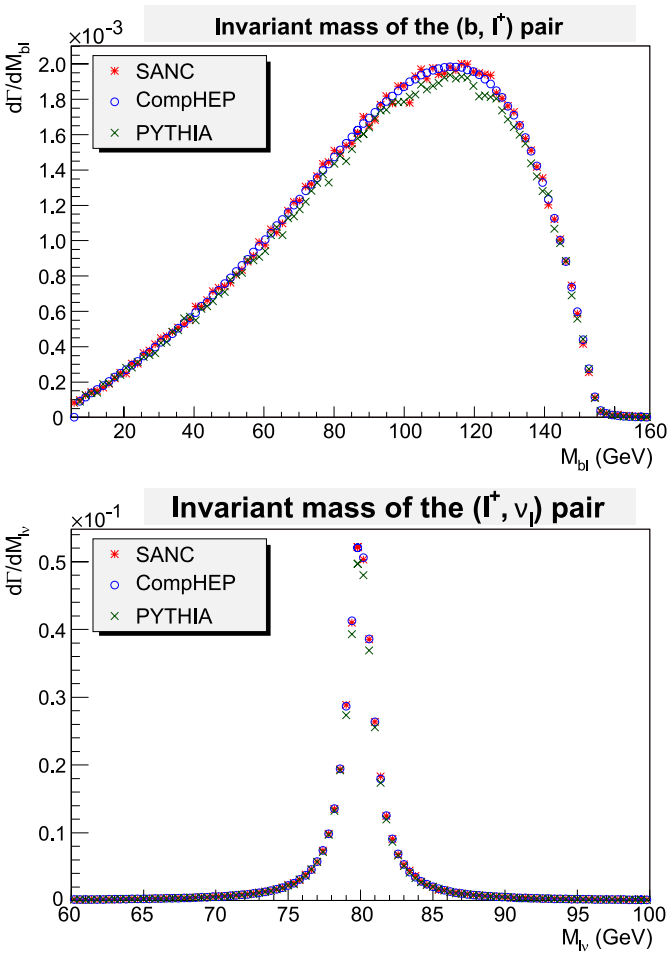

Fig. 4. Differential distributions for the process $t\to b\mu^+\nu_\mu$ of the invariant masses of the $b\mu^+$ and $\mu^+\nu_\mu$ pairs produced by SANC, CompHEP and PYTHIA

4 Radiative corrections

Radiative corrections can be subdivided into two parts: *virtual (one-loop)* corrections and *real (single photon emission)*. The latter, in turn, is subdivided into *soft* and *hard* photon emission; see (1).

4.1 Virtual corrections

Virtual corrections can be schematically represented by building block diagrams: dressed vertices, self-energies and boxes; see Fig. 5. They all, except the boxes, include relevant counterterm contributions in the same spirit as described for the neutral current (NC) case in [26]. We also apply the recipe of [27] to regularize the so-called "on-mass-shell" singularities.

The virtual contribution is parameterized by scalar form factors that can be found in the "SANC Output window" after a run of the FF-module on the top decay branch of the SANC tree; see Fig. 1.

4.2 Real corrections

The soft contribution is proportional to the Born level decay rate and has the same phase space. Its explicit expression can also be found in the "SANC Output window" after a SANC-run of the BR-module; see Fig. 1.

For hard photon emission there are four tree-level Feynman diagrams (see Fig. 6). One diagram corresponds to emission from the initial state, two diagrams describe the final state radiation, and the remaining diagram corresponds to radiation from the intermediate W^+ boson.

Hard bremsstrahlung in $t(p_1) \to b(p_2) + l^+(p_3) + \nu_l(p_4) + \gamma(p_5)$ has the four-body phase space:

$$\mathrm{d}\Phi^{(4)} = \Phi_1^{(2)}\,\mathrm{d}\Phi_2^{(2)}\,\mathrm{d}\Phi_3^{(2)}\,\frac{\mathrm{d}s_{25}}{2\pi}\,\frac{\mathrm{d}s_{34}}{2\pi}\,, \tag{8}$$

where the three two-body phase spaces are

$$\Phi_1^{(2)} = \frac{1}{8\pi}\,\frac{\sqrt{\lambda\,(m_t^2, s_{25}, s_{34})}}{m_t^2}\,,$$
$$\mathrm{d}\Phi_2^{(2)} = \frac{1}{8\pi}\,\frac{\sqrt{\lambda\,(s_{25}, m_b^2, 0)}}{s_{25}}\,\frac{1}{2}\,\mathrm{d}\cos\theta_1\,,$$

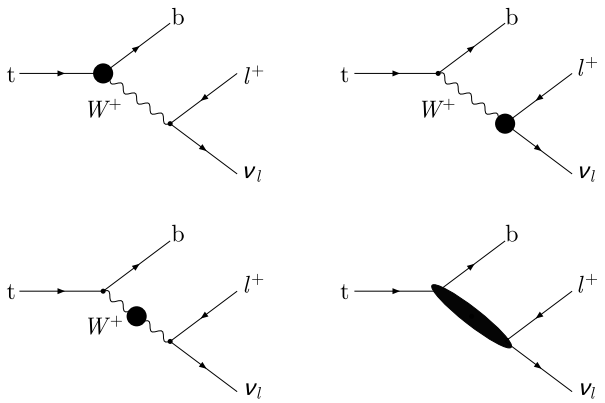

Fig. 5. Feynman diagrams for one-loop level decay

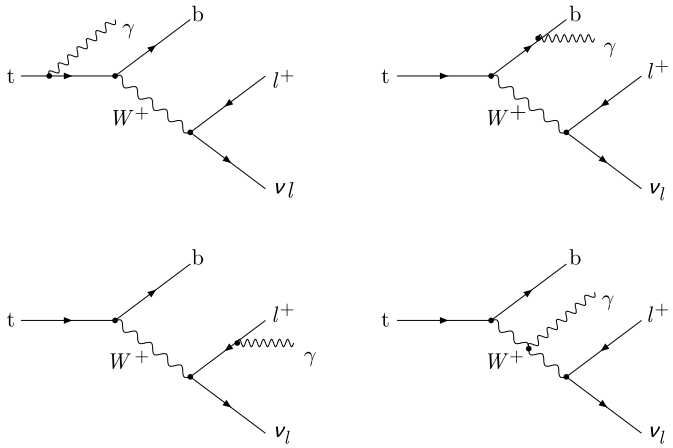

Fig. 6. Feynman diagrams for hard photon emission

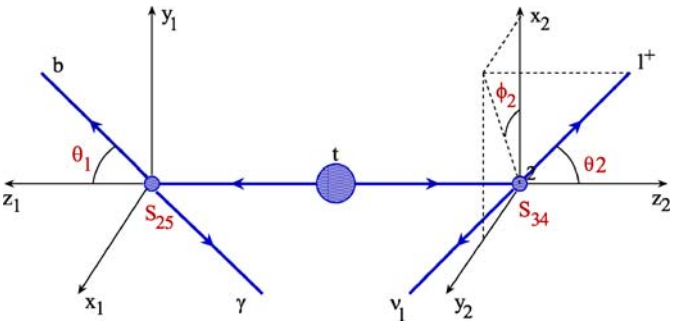

Fig. 7. Kinematical diagram for hard photon emission

$$\mathrm{d}\Phi_3^{(2)} = \frac{1}{8\pi}\,\frac{\sqrt{\lambda\,(s_{34}, m_l^2, 0)}}{s_{34}}\,\frac{1}{2}\,\mathrm{d}\cos\theta_2\,\mathrm{d}\phi_2\,. \tag{9}$$

The kinematics and meaning of the variables are illustrated in Fig. 7.

The total decay rate for the hard process is represented by a 5-fold integral over s_{25}, s_{34}, $\cos\theta_1$, $\cos\theta_2$, and ϕ_2, varying within the following limits:

$$\begin{aligned} m_b^2 &\le s_{25} \le (m_t - m_l)^2\,,\\ m_l^2 &\le s_{34} \le (m_t - \sqrt{s_{25}})^2\,,\\ -1 &\le \cos\theta_1 \le +1\,,\\ -1 &\le \cos\theta_2 \le +1\,,\\ 0 &\le \phi_2 \le 2\pi\,. \end{aligned} \tag{10}$$

The matrix element of Fig. 6 and the kinematics described in this section are the basis for the SANC Monte Carlo generator.

5 Numerical results

5.1 Comparison of hard bremsstrahlung between SANC and CompHEP

We begin by presenting the results of the Monte Carlo integration of the hard photon contributions derived with the help of SANC and CompHEP as presented in Table 2.

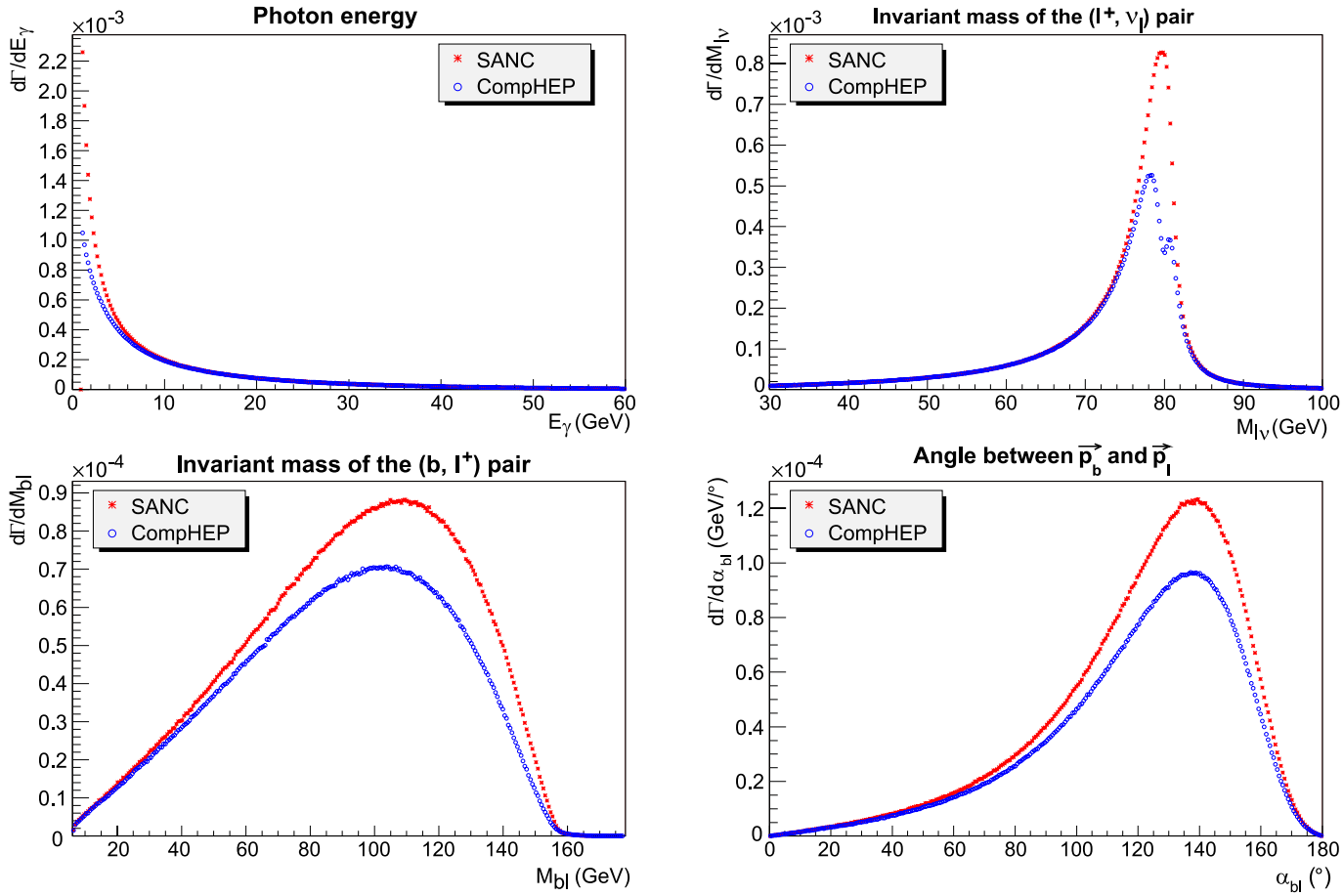

Fig. 8. Differential distributions for the hard photon emission process $t \to b\mu^+\nu_l\gamma$ with $E_\gamma \geq 1$ GeV

Table 2. Comparison for hard emission produced by the SANC and CompHEP systems for $E_\gamma \geq \bar{\omega}$

$\bar{\omega}$, GeV	$\Gamma^{\rm hard}$, 10^{-2} GeV CompHEP	$\Gamma^{\rm hard}$, 10^{-2} GeV SANC
10	0.2578(2)	0.2592(2)
1	0.6982(3)	0.8582(2)
10^{-1}	0.8538(3)	1.5000(3)
10^{-2}	0.9628(4)	2.1495(3)
10^{-3}	1.0730(4)	2.8005(4)
10^{-4}	1.1809(3)	3.4525(4)

There is a significant difference between the two sets of numbers, and this difference increases with decreasing $\bar{\omega}$. This difference is due to the approximate representation of the W boson propagators implemented in CompHEP; in CompHEP the complex propagator is used in a real representation:[1]

$$\frac{1}{p^2 - M_W^2 + \mathrm{i}M_W\Gamma_W} \to \frac{p^2 - M_W^2}{(p^2 - M_W^2)^2 + M_W^2\Gamma_W^2}\,. \tag{11}$$

[1] Here as an exception we use the metric $p^2 = M^2$.

This assumption will not lead to a noticeable departure from the correct result with the exception of the case in which we have the product of two different W propagators (i.e. with different virtualities). In this case, it is necessary to make a substitution that corrects this assumption:

$$\frac{p_1^2 - M_W^2}{(p_1^2 - M_W^2)^2 + M_W^2\Gamma_W^2}\,\frac{p_2^2 - M_W^2}{(p_2^2 - M_W^2)^2 + M_W^2\Gamma_W^2} \to$$
$$\frac{p_1^2 - M_W^2}{(p_1^2 - M_W^2)^2 + M_W^2\Gamma_W^2}\,\frac{p_2^2 - M_W^2}{(p_2^2 - M_W^2)^2 + M_W^2\Gamma_W^2}$$
$$+\,\frac{M_m^2\Gamma_W^2}{\left((p_1^2 - M_W^2)^2 + M_W^2\Gamma_W^2\right)\left((p_2^2 - M_W^2)^2 + M_W^2\Gamma_W^2\right)}\,. \tag{12}$$

We can explicitly observe the difference in Fig. 8, where we present the various differential distributions. As indicated in the upper two pictures the difference is to be seen in the region of soft photon emission near the resonance.

Note that if we use the recipe (11) in SANC, then we simulate the CompHEP distributions with a very good precision.

Table 3. Born and one-loop decay width and percentage of the correction in the α scheme

l	$\Gamma^{\rm Born}$, GeV	$\Gamma^{\rm 1\text{-}loop}$, GeV	δ, %
l^+	0.14948(1)	0.16064(1)	7.47

Table 4. Born and one-loop decay width and percentage of the correction in the $G_{\rm F}$ scheme

l	$\Gamma^{\rm Born}$, GeV	$\Gamma^{\rm 1\text{-}loop}$, GeV	δ, %
l^+	0.16018(1)	0.16299(1)	1.75

5.2 Numerical results for the complete EWRC

The results for the complete one-loop calculation of widths in the α and $G_{\rm F}$ schemes and comparison with Born level widths are presented in Tables 3 and 4.[2]

There is practically no sensitivity to the lepton mass, since it is neglected everywhere but in the arguments of logs which, in turn, are vanishing due to the Kinoshita–Lee–Nauenberg theorem.

6 EWRC in cascade approximation

It is interesting to compare results of the complete approach with an approximate, "cascade" calculation based on the formula (we consider the case $l = e$):

$$\Gamma_{t\to be\nu} = \frac{\Gamma_{t\to Wb}\Gamma_{W\to e\nu}}{\Gamma_W}\,. \tag{13}$$

The input parameters are as in (2), except m_b, which is set to zero here, and we present our results in the α and $G_{\rm F}$ schemes. Consider first the validity of (13) at the Born level for a (*formal*) variation of Γ_W; see Table 5.

The cascade approximation at the Born level improves rapidly with decreasing Γ_W.

Complete one-loop calculations are shown in Tables 6 and 7.

Now turn to the one-loop version of cascade (13). First, compute $\Gamma(t\to Wb)$ and $\Gamma(W\to e\nu)$ neglecting Γ_W in all W boson propagators (11). So in (13) the numerator does not depend on Γ_W. In this "naive" variant of the calculations it is sufficient to consider only one point over Γ_W, since the correction δ is a constant by construction.

From Tables 6–9 one sees that the complete and cascade one-loop calculations deviate considerably. This hints to effects of Γ_W in cascade calculations, which should be taken in account more carefully.

Having come to the end of this section, we note that the percentage of EWRC correction for $t\to Wb$ decay reasonably agrees with results given in Table 1 of [7], even though we did not tune any parameters to achieve agreement.

[2] Note carefully that although SANC may produce all results exactly in b-mass, all numbers in this subsection and Sect. 6 are derived for $m_b \to 0$.

Table 5. Comparison of Born widths without and with cascade approximation, $\alpha(0)$ scheme

	$\Gamma^{\rm Born}$, GeV	$\Gamma^{\rm Born}_{\rm cascade}$, GeV	δ, %
Γ_W	0.14948	0.15187	1.6
$\Gamma_W/10$	1.5163	1.5187	0.2
$\Gamma_W/10^2$	15.185	15.187	0.01
$\Gamma_W/10^3$	151.87	151.87	0.00

Table 6. Born and one-loop decay width and percentage of the correction, $\alpha(0)$ scheme

l	$\Gamma^{\rm Born}$, GeV	$\Gamma^{\rm 1\text{-}loop}$, GeV	δ, %
Γ_W	0.14949	0.16064	7.46

Table 7. Born and one-loop decay width and percentage of the correction, $G_{\rm F}$ scheme

l	$\Gamma^{\rm Born}$, GeV	$\Gamma^{\rm 1\text{-}loop}$, GeV	δ, %
Γ_W	0.16018	0.16299	1.75

Table 8. Born, one-loop decay widths and percentage of the correction in cascade approximation, $\alpha(0)$ scheme

	$t\to Wb$	$W\to e\nu$	$t\to be\nu$ cascade
$\Gamma^{\rm Born}$, GeV	1.4800	0.21970	0.15187
$\Gamma^{\rm 1\text{-}loop}$, GeV	1.5466	0.22528	0.16274
δ, %	4.49	2.54	7.15

Table 9. Born, one-loop decay widths and percentage of the correction in cascade approximation, $G_{\rm F}$ scheme

	$t\to Wb$	$W\to e\nu$	$t\to be\nu$ cascade
$\Gamma^{\rm Born}$, GeV	1.5321	0.22742	0.16274
$\Gamma^{\rm 1\text{-}loop}$, GeV	1.5572	0.22670	0.16488
δ, %	1.64	–0.32	1.31

7 Conclusions

A study of the semileptonic top quark decay $t\to bl^+\nu_l(\gamma)$ was presented. We have computed the total one-loop electroweak corrections to this process with the aid of the SANC system. Using a Monte Carlo integrator and an event generator that we have created for this purpose, we specify the influence on the decay width due to EWRC. These corrections are about 7.5% for the α scheme and approximately 1.8% for the $G_{\rm F}$ scheme. The comparison with the numbers of CompHEP and PYTHIA packages was done at the tree level. On comparison we found a notice-

able deviation from the CompHEP package for soft photon emission in the resonance region.

We have studied the cascade approach to the problem under consideration. We have shown that the "naive" approach with "stable" Ws is not precise enough. An improved treatment of the cascade approach with complex W-mass will be presented elsewhere.

Acknowledgements. This work was partly supported by the RFBR grant 07-02-00932 (AA, DB, SB, LK and RS) by the RF President grant 5332.2006 (AA) and by the EU grant mTkd-CT-2004-510126 in partnership with the CERN Physics Department and by the Polish Ministry of Scientific Research and Information Technology grant No. 620/E-77/6.PRUE/DIE 188/2005-2008 (GN). AA, DB, SB, LK and GN are indebted to the directorate of IFJ, Krakow, for hospitality that was extended to them in April–May 2005, when an essential part of this study was done.

References

1. A. Andonov et al., Comput. Phys. Commun. **174**, 481 (2006)
2. A. Arbuzov et al., Eur. Phys. J. C **46**, 407 (2006)
3. D. Bardin, S. Bondarenko, L. Kalinovskaya, G. Nanava, L. Rumyantsev, W. von Schlippe, "SANCnews: Sector $ffbb$", hep-ph/0506120
4. ATLAS detector and physics performance Technical Design report, Volume II, 1999
5. A. Andonov, A. Arbuzov, S. Bondarenko, P. Christova, V. Kolesnikov, R. Sadykov, QCD branch in SANC, hep-ph/0610268
6. A. Andonov, A. Arbuzov, S. Bondarenko, P. Christova, V. Kolesnikov, R. Sadykov, Part. Nucl. Lett. **4**, 6 (2007) [in press]
7. A. De nner, T. Sack, Nucl. Phys. B **358**, 46 (1991)
8. G. Eilam, R.R. Mendel, R. Migneron, A. Soni, Phys. Rev. Lett. **66**, 3105 (1991)
9. B.A. Irwin, B. Margolis, H.D. Trottier, Phys. Lett. B **256**, 533 (1991)
10. T. Kuruma, Z. Phys. C **57**, 551 (1993)
11. B. Lampe, Nucl. Phys. B **454**, 506 (1995)
12. S.M. Oliveira, L. Brucher, R. Santos, A. Barroso, Phys. Rev. D **64**, 017 301 (2001)
13. M. Fischer, S. Groote, J.G. Korner, M.C. Mauser, Phys. Rev. D **65**, 054 036 (2002)
14. H.S. Do, S. Groote, J.G. Korner, M.C. Mauser, Phys. Rev. D **67**, 091 501 (2003)
15. B.H. Smith, M.B. Voloshin, Phys. Lett. B **340**, 176 (1994)
16. S. Mrenna, C.P. Yuan, Phys. Rev. D **46**, 1007 (1992)
17. K.G. Chetyrkin, R. Harlander, T. Seidensticker, M. Steinhauser, hep-ph/9910339
18. M. Slysarczyc, Two-loop QCD corrections to top quark decay, Lake Louise 2004, Fundamental interactions, hep-ph/0401026, pp. 284–288
19. Q.H. Cao, C.P. Yuan, Phys. Rev. Lett. **93**, 042 001 (2004)
20. CompHEP Collaboration, E. Boos et al., Nucl. Instrum. Methods A **534**, 250 (2004)
21. T. Sjöstrand, S. Mrenna, P. Skands, JHEP **0605**, 026 (2006)
22. J.A.M. Vermaseren, New features of FORM, math-ph/0010025
23. D. Bardin, G. Passarino, The Standard Model in the Making: Precision Study of Electroweak Interactions (Oxford, Clarendon, 1999)
24. http://pdg.lbl.gov/2006/tables/contents_tables.html
25. G.P. Lepage, J. Comput. Phys. **27**, 192 (1978)
26. A. Andonov et al., Phys. Part. Nucl. **34**, 577 (2003) [Fiz. Elem. Chast. Atom. Yadra **34**, 1125 (2003)]
27. D. Wackeroth, W. Hollik, Phys. Rev. D **55**, 6788 (1997)